Numerical Analysis of Effect of Surface Active Elements on Marangoni Flow in Melt Pool

K. Yadav[1*] and A. Mishra[1]
[1]Indian Institute of Technology, Kanpur
*Corresponding author: Indian Institute of Technology Kanpur, Kanpur-208016, India.
Email address: kulydv@iitk.ac.in

Abstract: Marangoni flow affects the heat and mass transfer occurring in the molten metal regions in welding and additive manufacturing processes. It originates from the surface tension gradient ($\partial\gamma/\partial T$) induced at the melt pool surface due to the temperature difference. The flow pattern within melt pool affects the segregation and melt-pool shape and size. The flow pattern and therefore the melt pool shape vary with the $\partial\gamma/\partial T$, which is dependent on both the temperature and the surface active elements concentration in the molten metal. Elements of the oxygen family, (O, S, Se and Te) are found to be strongly surface active. In the present study, numerical modeling and simulation is used to show the dependence of flow field and resulting melt pool shape on the surface active elements. Stainless steel alloy has been used as base for the modeling and sulfur is studied as the surface active element. The numerical modeling has been done using COMSOL Multiphysics 5.2 software.

Keywords: COMSOL Multiphysics, Marangoni flow, Surface active elements, Surface tension, Surfaced temperature gradient, Melt pool.

1. Introduction

Marangoni flow significantly affects the heat and mass transportation phenomena in Welding and Additive Manufacturing processes. The flow affects the melt pool evolution, segregation, melt pool depth as well as the final microstructure and mechanical properties.

Marangoni flow is induced by the surface tension gradient that results from the temperature gradient at the melt pool surface. The flow occurs from the low to high surface tension regions, and therefore establishes a circulating motion within the melt pool. This motion transports heat and mass from hotter regions to colder regions within the melt pool. The intensity and direction of the flow and the accompanying heat and mass transfer are strongly dependent on the surface tension gradient.

The magnitude and direction of the Marangoni flow in the melt pool are related to the Marangoni number (Ma) defined as

$$Ma = \left(\frac{\partial\gamma}{\partial T}\right)\left(\frac{\partial T}{\partial x}\right)\frac{L^2}{\mu\alpha} \quad (1)$$

Where $\partial T/\partial x$ is the temperature gradient along the surface, μ and α dynamic viscosity and thermal diffusivity of the molten metal and L is the characteristic length (radius of pool). The Marangoni number is a dimensionless number showing relative importance of surface tension forces to viscous forces. For welding and SLM operations, $\partial\gamma/\partial T$ term is of great importance. Although the values are small (~10^{-4} to 10^{-3}), still the value as well as sign would have crucial effect on the weld pool geometry.

Presence of surface active impurities within the molten metal may cause the surface tension gradient become positive. Among the different impurities present in the molten metal, the group VI elements (O, S, Se, Te) are most important, specially S and O, as they are most strongly surface active.

The dependence of surface tension gradient of an alloy on both temperature and activity of a component can be expressed by the following equation (Mcnallan and Debroy, 1991)

$$\frac{\partial\gamma}{\partial T} = -A - R\Gamma_s \ln(1 + Ka_i) - \left(\frac{Ka_i}{1 + Ka_i}\right)\left(\frac{\Gamma_s \Delta H°}{T}\right) \quad (2)$$

Where A is a coefficient for the variation of surface tension at temperature T above the liquidus temperature, R= 8.314J/mol-K is the gas constant, Γ_s is the surface excess at saturation (kg-mole/m^2), K is the entropy segregation constant, and $\Delta H°$ is the enthalpy of segregation (kJ/kg), a_i is the activity of species i in solution. However, a major limitation of these equations is that they are applied only for one element at a time.

From the equation (2), it is obvious that the surface tension gradient change with increasing temperature and surface active impurity concentration.

The surface tension gradient decreases with temperature when the surface active elements concentration is low. So the surface tension decreases with temperature, rendering hotter central region at lower surface tension than the cooler edge regions. This results in wide and shallow melt pools, because the molten metal flows outwards from the center to the edges. As the surface active element concentration increases, the surface temperature gradient starts increasing. When the surface active elements' concentration increase to such an extent, that the surface tension gradient becomes positive for the whole region, the flow pattern reverses completely and result in a deep and narrow melt pool.

Hence the study of surface tension dependence on both temperature and concentration of surface active elements is prerequisite and of ultimate importance to understand the melt pool evolution and resulting flow patterns and segregation.

In the present study, 2-D numerical modeling of marangoni convection has been done using COMSOL Multiphysics for the laser spot welding of stainless steel to study the flow pattern changes. The variations in the surface tension gradient due to changing concentration of sulfur are taken into account. The resultant melt pool evolution has been studied, and the melt pool depths are obtained through the simulation results for different cases. The simulation results are compared to the experimental results from available literature.

Mathematical modeling:

(I) Governing equations:

To simplify the mathematical model, some assumptions are made:

(1) Incompressible, laminar and Newtonian flow due to smaller weld pool size
(2) Constant physical properties of liquid and solid metal
(3) Gaussian beam profile of the heat source
(4) Boussinesq approximation valid.

The governing equations include the continuity, momentum and energy equations for two-dimensional case,

Continuity equation:

$$\frac{\partial \rho u}{\partial x} + \frac{\partial \rho v}{\partial y} = 0 \tag{3}$$

Momentum equation (x-direction):

$$-\frac{\partial(\rho u_x v)}{\partial x} + \frac{\partial \rho u u}{\partial x} + \frac{\partial \rho v u}{\partial y} = -\frac{\partial P}{\partial x} + \frac{\partial}{\partial x}\left(\frac{\mu \partial u}{\partial x}\right) + \frac{\partial}{\partial y}\left(\frac{\mu \partial u}{\partial y}\right) + Sx \tag{4}$$

Momentum equation (y-direction):

$$-\frac{\partial(\rho u_x v)}{\partial x} + \frac{\partial \rho u v}{\partial x} + \frac{\partial \rho v v}{\partial y} = -\frac{\partial P}{\partial y} + \frac{\partial}{\partial x}\left(\frac{\mu \partial v}{\partial x}\right) + \frac{\partial}{\partial y}\left(\frac{\mu \partial y}{\partial y}\right) + Sy \tag{5}$$

Energy equation:

$$-\frac{\partial}{\partial x}(\rho u_x H) + \frac{\partial}{\partial x}(\rho u H) + \frac{\partial}{\partial y}(\rho v H) = \frac{\partial}{\partial x}\left(K\frac{\partial T}{\partial x}\right) + \frac{\partial}{\partial y}\left(K\frac{\partial T}{\partial y}\right) + S_H \tag{6}$$

Where u_x- the welding speed, ρ- density, *K*-thermal conductivity, μ- viscosity, P pressure and H is the enthalpy.

The source terms S*x*, S*y*, and S_H are given below

Momentum source term in x-direction:

$$S_x = -\frac{C(1-f_l)^2}{b + f_l^3} u \tag{7}$$

Momentum source term in y-direction:

$$S_y = \rho g \beta (T - T_m) - \frac{C(1-f_l)^2}{b + f_l^3} v \tag{8}$$

Here the $\rho g \beta (T - T_m)$ term is the boussinesq approximation for the buoyancy forces. The second term is for the flow within the mushy zone. The variable f_l is the liquid fraction, defined as

$$f_l = \begin{cases} 0 & T \le T_s \\ \dfrac{T - T_s}{T_l - T_s} & T_s < T < T_l \\ 1 & T > T_l \end{cases}$$

Energy source term is,

$$S_H = -\left(\frac{\partial}{\partial x}(\rho u \Delta H) + (\frac{\partial}{\partial y}(\rho v \Delta H)\right) + \frac{\partial}{\partial x}(\rho u_x \Delta H) \quad (9)$$

Where $\Delta H = F(T)$the latent heat content, is defined as a function of temperature T and is given by

$$F(T) = \begin{cases} L & T < T_l \\ \dfrac{T - Ts}{T - Tl} L & T_s \le T \le T_l \\ 0 & T < T_s \end{cases}$$

Where L = latent heat, T_l = liquidus temperature and T_s = solidus temperature

(II) Boundary conditions

The model considers a surface heat source (laser beam) with Gaussian distribution,

$$q_{in} = \frac{2P}{\pi r^2} \exp\left(-\frac{2x^2}{r^2}\right)$$

Where P = laser power and r = spot radius of laser beam

On the surface there will be heat loss due to both convection and radiation, however, the convective losses are omitted due to weld pool being very small and the radiation losses being proportional to T^4.

So at the top surface there will be a heat loss,

$$q_{loss} = -\varepsilon\sigma(T^4 - T_a^4)$$

T_a= the ambient temperature, ε = emissivity of the surface and σ = the Stefan-Boltzmann constant.

On the free surface of the melt pool,

$$\mu \frac{\partial u}{\partial y} = -\frac{\partial T}{\partial y}\frac{\partial \gamma}{\partial T}$$

Here $\frac{\partial \gamma}{\partial T}$ is the surface tension gradient. The effect of surface active elements on the melt pool can now be accessed by using the expression for the surface tension gradient, i.e. equation (2)

$$\frac{\partial \gamma}{\partial T} = -A - R\Gamma_s \ln(1 + Ka_i) - \left(\frac{Ka_i}{1 + Ka_i}\right)\left(\frac{\Gamma_s \Delta H^\circ}{T}\right)$$

And

$$K = K_1 \exp\left(\frac{-\Delta H^\circ}{RT}\right) \quad (10)$$

(III) Numerical modeling:

For a thorough understanding of the dependence of flow pattern and resulting melt pool shape evolution on the surface tension gradient, numerical modeling is done using COMSOL 5.2. Since the gradient value depends on the temperature and the concentration of surface active elements, their effect also has to be accounted during modeling. This is done by including equation (2) along with the governing equations of continuity, momentum and energy equations in the numerical model.

The thermal and physical properties of the alloy used for the numerical model are given in the table 1.

Table.1. Thermal and physical properties of stainless steel alloy used in the study

Solidus temperature	1670 K
Liquidus temperature	1723 K
Density	7200 kg/m^3
Thermal conductivity	22 W/mK
Coefficient of thermal expansion	10^{-4} K^{-1}
Specific heat capacity	702 J/kg-K
Latent heat of melting	267.5 kJ/kg
Radiation emissivity	0.4
Dynamic viscosity	0.006 (Pa-s)

For the sake of easy and clear understanding, a two-dimensional model of laser spot melting has been built in COMSOL. The model is of rectangular shape with dimensions 4 mm x 2 mm. The laser power is taken as 25 W; the beam spot diameter is 126 μm. A Gaussian beam profile is chosen for the laser beam.

Results:

Numerical simulations are run for two cases. First a number of simulations are run to show how the flow pattern and therefore the melt pool shape evolve with the surface tension gradient ∂γ/∂T as its sign changes from negative to positive. Figs. 1(a) to 1(f) show the flow pattern

and melt pool shape for $\partial\gamma/\partial T$ values in range of ± 0.005 N/mK with steps taken of 0.002 N/mK. The flow occurs from center towards the melt pool edges (outwards flow) when $\partial\gamma/\partial T$ = -0.005 N/mK. As the $\partial\gamma/\partial T$ increases, the outward flow diminishes gradually, as shown in the 1(b) and 1(c) cases, where $\partial\gamma/\partial T$ is taken -0.003and -0.001 N/mK respectively.

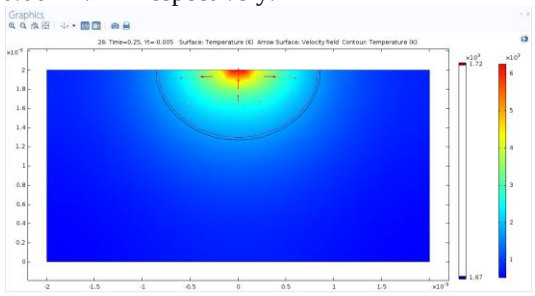

Figure 1(a). $\partial\gamma/\partial T$= -0.005 N/mK

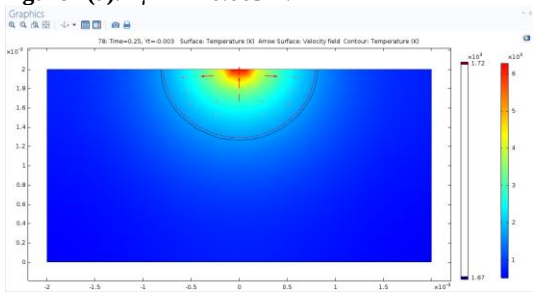

Figure 1(b). $\partial\gamma/\partial T$= -0.003 N/mK

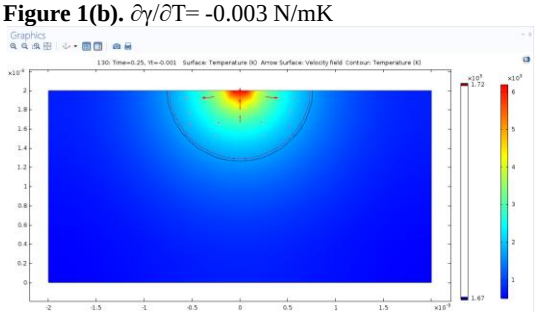

Figure 1(c). $\partial\gamma/\partial T$= -0.001 N/mK

As soon as the $\partial\gamma/\partial T$ becomes positive, the flow reverses, and an inward flow is seen from the edges to the center. As the $\partial\gamma/\partial T$ increases further, the inwards flow intensity increases. This can be seen in figs. 1(d), (e) and (f). The melt pool shape at negative $\partial\gamma/\partial T$ is wide and shallow, which becomes narrow and deep as $\partial\gamma/\partial T$ becomes positive. The melt pool depth increases as the gradient increases.

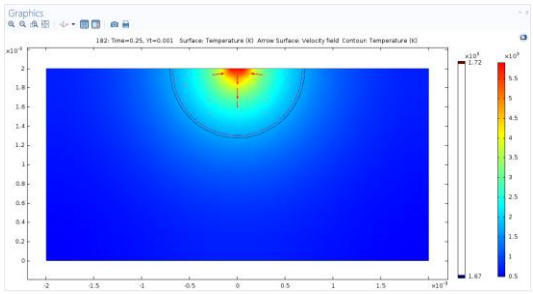

Figure 1(d). $\partial\gamma/\partial T$= 0.001 N/mK

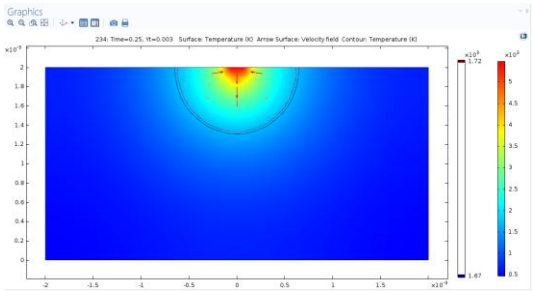

Figure 1(e). $\partial\gamma/\partial T$= 0.003 N/mK

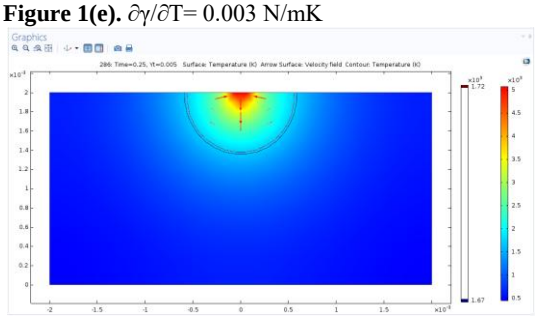

Figure 1(f). $\partial\gamma/\partial T$= 0.005 N/mK

When surface tension gradient is negative, the center of the melt pool is at low pressure and outer regions are at higher pressure, as can be seen in the fig. 2(a). This pressure difference causes the melt to flow from the outer regions to the center in the bulk of melt pool, and transports cooler metal to hotter central regions.

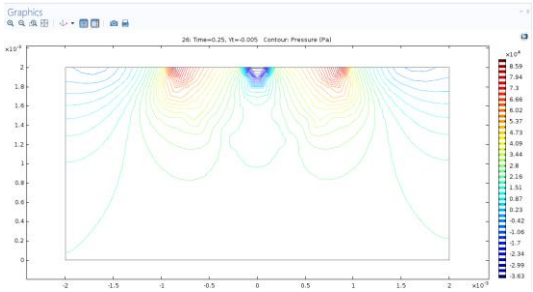

Figure 2(a). Pressure field in melt pool for $\partial\gamma/\partial T$ = -0.005 N/mK

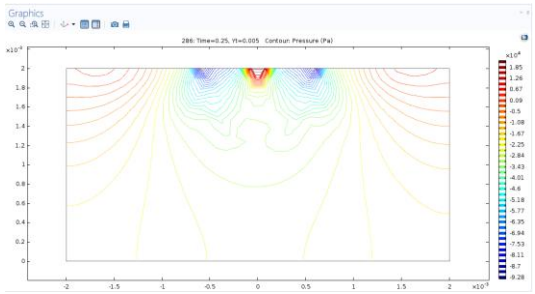

Figure 2(b). Pressure field for $\partial\gamma/\partial T$ = 0.005 N/mK

As the surface tension gradient becomes positive, the pressure field reverses creating a high pressure region at the center of the melt pool, and low pressure region at the outer regions. This pressure difference causes the melt to flow from the central region to outer regions in bulk of the melt pool. This along with the inwards flow on the top surface establishes a counter clockwise circulating flow within the melt pool. This can be seen in the fig 2(b).

Next, simulations are done to show the dependence of surface tension gradient $\partial\gamma/\partial T$ on the concentration of surface active elements. An example case of sulfur in steel is taken. The properties of alloy are same as given in table 1. The eqn. (2) along with eqn. (10) is used, with coefficients and constants of eqn. (2) and (10) given below

$A=4.3\times10^{-4}$ N/mK, R=8314.3 J/kg.mol.K

$\Gamma_s= 1.3\times10^{-7}$ kg-mol/m^2, $K_1= 3.18\times10^{-3}$,

$\Delta H^o =-188\times10^3$ kJ/kg-mol,

a_i= activity of sulfur (% S)

Using these values in the equation (2), the surface tension gradient is obtained as

$$\frac{\partial\gamma}{\partial T} = -4.3x10^{-4} - 1.808x10^{-3}\ln(1+Ka_i) + \frac{Ka_i}{1+Ka_i}\left(\frac{24.4}{T}\right) \qquad (11)$$

Where, $K = 3.18x10^{-3}\exp\left(\frac{22612.14}{T}\right)$ (12)

From equations (11) and (12), it is clear that the surface tension gradient $\partial\gamma/\partial T$ is only function of temperature and %mass fraction of sulfur. The plot of surface tension gradient $\partial\gamma/\partial T$ vs. T for different % mass fraction of S is shown in figs. 3(a) to (d).

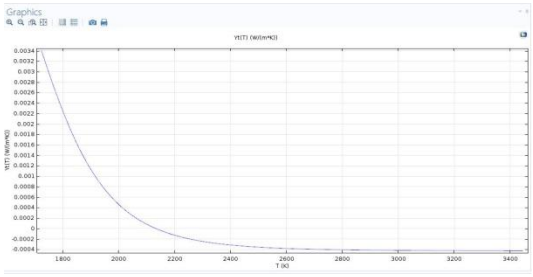

Figure 3(a). $\partial\gamma/\partial T$ vs. T, 0.0005 % S

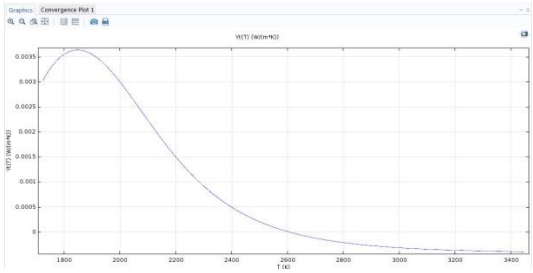

Figure 3(b). $\partial\gamma/\partial T$ vs. T, 0.005 % S

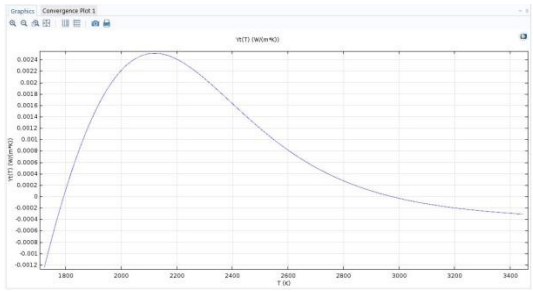

Figure 3(c). $\partial\gamma/\partial T$ vs. T, 0.02 % S

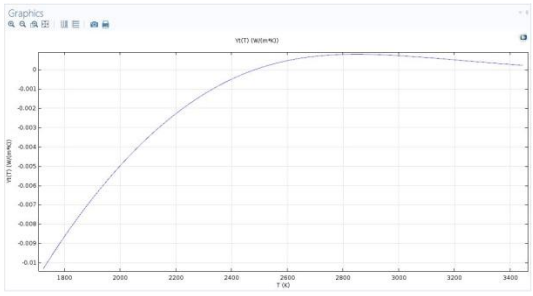

Figure 3(d). $\partial\gamma/\partial T$ vs. T, 0.2 % S

The variation of $\partial\gamma/\partial T$ with temperature is dependent upon the % mass fraction of sulfur.

When the sulfur concentration is low (fig.3(a)), the $\partial\gamma/\partial T$ is positive at low temperatures and decreases continuously with increasing temperature eventually becoming negative after temperature T~ (2150K).

As the S concentration increases the $\partial\gamma/\partial T$ vs. T curve has a point of inflection. At low

temperatures, the $\partial\gamma/\partial T$ is negative and continues to increase with temperature (fig. 3(b), (c)) till a temperature at which the curve reaches maxima. When the temperature increases beyond this value, $\partial\gamma/\partial T$ starts decreasing and becomes zero at a certain temperature, for example at 2600 K in the fig. 3(b). Beyond this temperature, the $\partial\gamma/\partial T$ becomes negative again.

Both the point of inflection in the $\partial\gamma/\partial T$ vs. T plot and the point at which $\partial\gamma/\partial T$ becomes zero shift towards higher temperatures as the sulfur concentration increases. This can be seen in the figs. 3(a),(b) and (c), where point of inflection shifts from 1850K (at 0.005%S) to 2100K (at 0.02%S) to 2850K (at 0.2%S), and the $T_{(\partial\gamma/\partial T=0)}$ shifts from 2600K (at 0.005%S) to 2950K (at 0.02%S) to 2900K (at 0.2%S).

(IV) Effect of sulfur concentration on the flow pattern within melt pool

Figures 4(a) to 4(e) shows the flow pattern evolution with increasing temperature as the $\partial\gamma/\partial T$ changes. The simulation results shown here correspond to the fig. 3(c), i.e. S mass fraction is 0.02%.

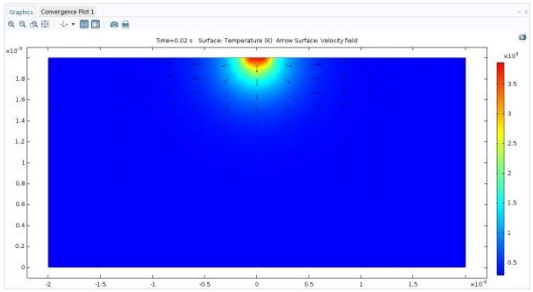

Figure 4(a). Flow pattern at t = 0.02 s

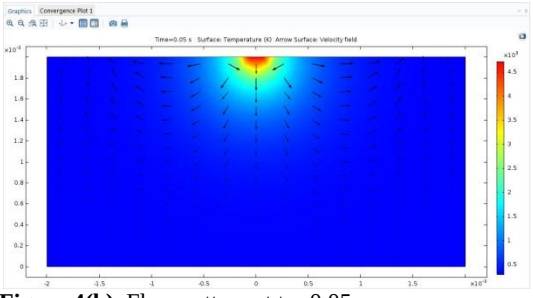

Figure 4(b). Flow pattern at t = 0.05 s

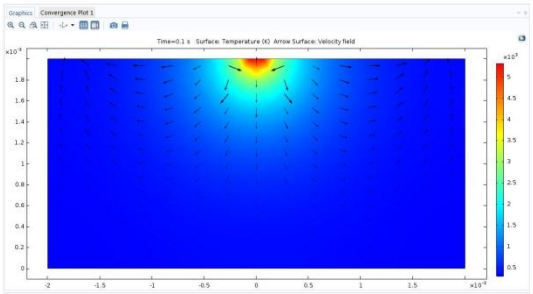

Figure 4(c). Flow pattern at t = 0.1 s

As shown in figs. 4(a) and (b), the flow is inwards when the peak temperature is low (~3000K). However, at t = 0.1 μs, the peak temperature becomes > 3000 K, and an opposing flow (outwards flow, locally negative $\partial\gamma/\partial T$) is started in the pool.

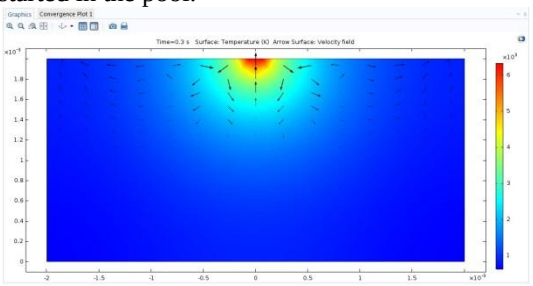

Figure 4(d). Flow pattern at t = 0.3 s

As the irradiation time increases, (at t= 0.3 s) an outwards flow is developed in the region where T> 3000K, while an opposing inwards flow is present in outside region where T< 3000K. This opposing flow fields further develop with time.

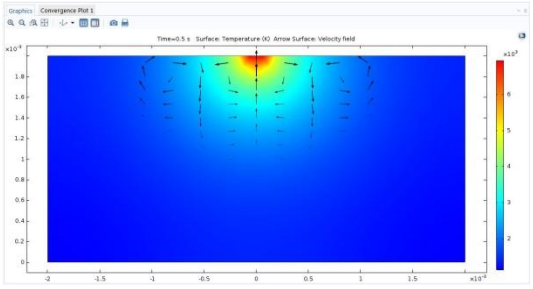

Figure 4(e). Flow pattern at t=0.5 s

At time t = 0.5 s, two opposing flow fields are clearly observable. In the central region flow is outwards corresponding to negative $\partial\gamma/\partial T$, while the surrounding regions have inwards flow corresponding to positive $\partial\gamma/\partial T$.

Conclusion:

Above results clearly show how the Marangoni flow develops due to presence of surface tension gradient at the melt pool surface. The evolution of melt pool shape and the dependence of flow pattern on the sign of surface tension gradient are discussed with the help of simulation results. Later, the dependence of surface tension gradient on the surface active elements concentration is analyzed and expressions are obtained for the surface tension gradient in terms of temperature and concentration of surface active element. Simulation results of flow fields are shown for a chosen concentration.

References:

1. M.J. McNallan, T. Debroy, Effect of Temperature and Composition on Surface tension in Fe-Ni-Cr alloys containing sulfur, Metallurgical and Materials Transactions B, (1991)
2. C.X. Zhao, C. Kwakernaak, Y. Pan, I.M. Richardson, Z. Saldi, S. Kenjeres, C.R. Kleijn, The effect of oxygen on transitional Marangoni flow in laser spot welding, Acta Materialia 58, 6345-6357, (2010)
3. Y. Zhao, Y. Lei, Y.Shi, Effects of surface active sulfur on flow patterns of welding pool, Journal of material science and technology, vol. 21, no. 3, (2004)
4. Y. Su, K.C. Mills, A model to calculate surface tension of commercial alloys, Journal of material science, 40, pp 2185-2190, (2005)
5. P.D. Lee, P.N. Quested, M. Mclean, 1998. Philosophical transactions of the Royal Society of mathematical, physical and engineering sciences. April, (1998)
6. S. Wang, R. Nates, T. Pasang, M. Ramezani, Modeling of Gas Tungsten Arc Welding under Marangoni convection, Universal journal of mechanical engineering 3(5), pp 185-201, (2015)
7. Y.S. Lee, M. Nordin, S.S. Babu, D.F. Farson, Influence of fluid convection on weld pool formation in laser cladding, welding journal, vol. 93, pp 293-300, (2014)